Research Article J. Electrochem. Sci. Technol., **2016**, 7(2), 153-160

Journal of Electrochemical Science and Technology
jecst.kecs.or.kr

Impedance Spectroscopy Studies on Corrosion Inhibition Behavior of Synthesized N,N'-bis(2,4-dihydroxyhydroxybenzaldehyde)-1,3-Propandiimine for API-5L-X65 Steel in HCl Solution

I. Danaee[1]*, N. Bahramipanah[2], S. Moradi[1], and S. Nikmanesh[1]
[1]*Abadan Faculty of Petroleum Engineering, Petroleum University of Technology, Abadan, Iran*
[2]*Department of Chemistry, Payame Noor University, P.O.BOX 19395-3697, Tehran, Iran*

ABSTRACT

The inhibition ability of N,N-bis(2,4-dihydroxyhydroxybenzaldehyde)-1,3-Propandiimine (DHBP) as a schiff base against the corrosion of API-5L-X65 steel in 1 M HCl solution was evaluated by electrochemical impedance spectroscopy, potentiodynamic polarization and scanning electron microscopy. Electrochemical impedance studies indicated that DHBP inhibited corrosion by blocking the active corrosion sites. The inhibition efficiency increased with increasing inhibitor concentrations. EIS data was analysed to equivalent circuit model and showed that the charge transfer resistance of steel increased with increasing inhibitor concentration whilst the double layer capacitance decreased. The adsorption of this compound obeyed the Langmuir adsorption isotherm. Gibbs free energy of adsorption was calculated and indicated that adsorption occurred through physical and spontaneous process. The corrosion inhibition mechanism was studied by potential of zero charge. Polarization studies indicated that DHBP retards both the cathodic and anodic reactions through adsorption on steel surface. Scanning electron microscopy was used to study the steel surface with and without inhibitor.

Keywords : Corrosion, Inhibitor, Steel X65, Schiff base, Impedance

Received : 23 March 2016, Accepted : 4 May 2016

1. Introduction

Even with advanced corrosion resistant materials available, steel has been widely employed as construction materials for pipe work in the oil and gas production such as down hole tubular, flow lines and transmission pipelines [1]. API 5L X65 steel is the most widely accepted material for these types of pipes [2,3]. Steel pipelines play an important role in transporting gases and liquids throughout the world. Acid solutions are widely used in industries for lots of purposes, such as acid pickling, industrial acid cleaning, acid descaling and oil well acidizing [4]. Due to the general aggressive nature of acid solutions, this leads to corrosive attack. Massive costs are invested to manage corrosion in the oil and gas industry. The strategies consist of either using corrosion resistant alloys or the use of steel with corrosion inhibitor [5].

Inhibition effect of organic compound inhibitors is due to the interaction between the inhibitor molecules and the metal surface via adsorption. The inhibitor adsorption depends on parameters such as the surface charge and nature of the metal, the inhibitor structure, aggressive media type and the extent of aggressiveness and also on the nature of its interaction with the metal surface [6]. Generally the organic compounds containing hetero atoms like O, N, S and P are found to work as very effective corrosion inhibitors [7]. The choice of the inhibitor is based on two considerations, firstly economic consideration and secondly, high inhibition efficiency. Both features obviously can be combined within the same molecule such as Schiff bases [8-10]. In the past few years, the corrosion inhibition of various metals such as aluminum, and steel in acid solutions by Schiff bases with envi-

*E-mail address: danaee@put.ac.ir
DOI: http://dx.doi.org/10.5229/JECST.2016.7.2.153

ronmental considerations has attracted more attention [11]. Schiff bases can conveniently be synthesized from relatively cheap starting materials, an amine and a ketone or aldehyde. It's also reported that, Schiff bases show more inhibition efficiency than the corresponding amine [12].

This work is devoted to study the inhibition characteristics of N,N'-bis(2,4-dihydroxyhydroxybenzaldehyde)-1,3-Propandiimine as an inhibitor for steel in HCl solution, using electrochemical impedance spectroscopy (EIS), potentiodynamic polarization and scanning electron microscopy. Potential of zero charge (PZC) was also determined to establish the corrosion inhibition mechanism.

2. Materials and Methods

2.1. Materials

API-5L-X65 samples were cut from parent pipe with chemical composition reported as C:0.12, Mn:1.3, Si: 0.22, Cr: 0.25, Mo: 0.18, Cu: 0.12, Ni: 0.1, P: 0.01, S: 0.003, Al: 0.02, Nb: 0.05, Sn: 0.01, V: 0.05, Ti: 0.005, and Fe: Rest. The specimens of dimension 1 cm × 1 cm (exposed) × 4.3 mm (isolated with polyester resin) were used for electrochemical methods. They were polished mechanically using different grade emery papers up to 2000, washed thoroughly with doubly distilled water, and degreased with acetone before being immersed in the acidic solution.

The DHBP Schiff base inhibitor (Fig. 1) was provided in high yield (97 %) by the condensation of 2,4-Dihydroxybenzaldehyde (2 mmol) with 1,3-diaminopropane (1 mmol) in a stirred ethanolic solution and heated to reflux for 4 h according to the described procedure [13]. The resulting precipitate was filtered off, washed with warm ethanol and diethyl ether. Identification of structure of synthesized Schiff base was performed by ^{1}HNMR spectroscopy and elemental analysis. The concentration range of inhibitor employed was varied from 1×10^{-4} to 2×10^{-3} M.

2.4. Apparatus and methods

The apparatus for electrochemical investigations consists of computer controlled Auto Lab potentiostat/galvanostat (PGSTAT302N) electrochemical measurement system. Potentiodynamic polarization was performed at a scan rate of 1 mV s^{-1}. The electrochemical experiments were carried out using a conventional three electrode cell assembly at 20 ± 2 °C. A rectangular platinum foil was used as counter electrode and saturated calomel electrode as the reference electrode. Open circuit potentials (OCP) were obtained by potentiostat/galvanostat. The EIS experiments were conducted in the frequency range of 100 kHz to 0.01 Hz at open circuit potential with AC potential amplitude 10 mV. Time interval of 20-25 min was given for steady state attainment of open circuit potential. The electrochemical impedance spectra were also recorded at different anodic and cathodic biased potentials other than open circuit potential and the double layer capacitance values were plotted against the applied DC potentials to determine PZC. The PZC has lowest capacitance value in variation of double layer capacitance versus applied anodic and cathodic potentials. Fitting of experimental impedance spectroscopy data to the proposed equivalent circuit was done by means of home written least square software based on Marquardt method for the optimization of functions and Macdonald weighting for the real and imaginary parts of the impedance [14,15].

For surface analysis, the specimens were immersed in 1 M HCl prepared with and without addition of 1×10^{-3} M inhibitor at 20±2 °C for 6 h, cleaned with distilled water. The surface morphology of steel was evaluated by scanning electron microscopy (VEGA\TESCAN).

3. Results and Discussion

3.1. Impedance spectroscopy

Fig. 2 shows the Nyquist diagrams of API-5L-X65 in 1 M HCl solutions containing different concentrations of DHBP. All the impedance spectra exhibit single

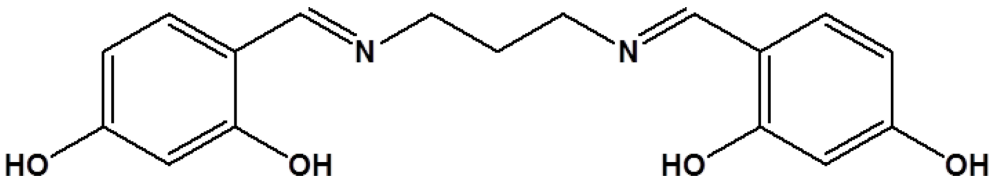

Fig. 1. Chemical structure of DHBP.

depressed semicircle due to the charge transfer resistance and double laye capacitance. The diameter of semicircle increases with the increase of DHBP concentrations. The addition of DHBP causes a remarkable decrease in the corrosion rate. These results are indicative of the adsorption of inhibitor molecules on the active sites of steel surface [16]. The inhibition of steel corrosion increases with increasing inhibitor concentrations. Moreover, the inhibition efficiencies show no considerable increase with concentrations of inhibitor higher than 2×10^{-3} M and almost are constant. The semicircular appearance shows that the corrosion of steel is controlled by the charge transfer and the presence of DHBP does not change the mechanism of steel dissolution [17,18]. In addition, these Nyquist diagrams are not perfect semicircles. The deviation of semicircles from perfect circular shape is often referred to the frequency dispersion of interfacial impedance [18-20]. This behaviour is usually attributed to the inhomogeneity of the metal surface arising from surface roughness or interfacial phenomena [20,21], which is typical for solid metal electrodes [22]. The equivalent circuit compatible with the Nyquist diagram recorded in the presence of inhibitor is depicted in Fig. 3. The simplest approach requires the theoretical transfer function $Z(\omega)$ to be represented by a parallel combination of a resistance R_{ct} and a capacitance C, both in series with another resistance R_s [23]:

$$Z(\omega) = R_s + \frac{1}{\frac{1}{R_{ct}} + i\omega C} \quad (1)$$

where is the frequency in rad/s, $\omega = 2\pi f$ and f is frequency in Hz. To obtain a satisfactory impedance simulation of steel, it is necessary to replace the capacitor (C) with a constant phase element (CPE) Q in the equivalent circuit. The most widely accepted explanation for the presence of CPE behavior and depressed semicircles on solid electrodes is microscopic roughness, causing an inhomogeneous distribution in the solution resistance as well as in the double layer capacitance [24]. Constant phase element Q_{dl}, R_s and R_{ct} can be corresponded to double layer capacitance $Q_{dl} = R^{n-1}C_{dl}^{n}$, solution resistance and charge transfer resistance, respectively. To corroborate the equivalent circuit, the experimental data are fitted to equivalent circuit and the circuit ele-

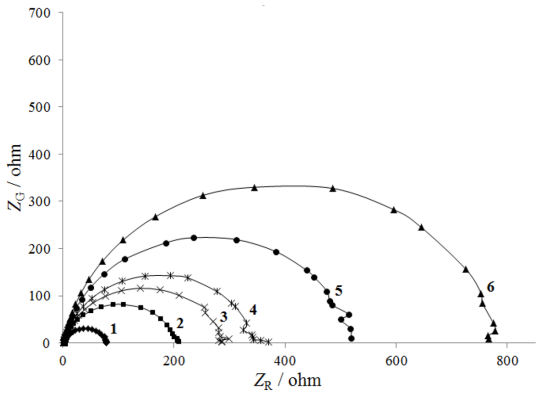

Fig. 2. Nyquist plots for steel in 1 M HCl without and with various concentration of DHBP at 20 °C: (1) 0, (2) 1×10^{-4}, (3) 3×10^{-4}, (4) 5×10^{-4}, (5) 1×10^{-3}, (6) 2×10^{-3} M.

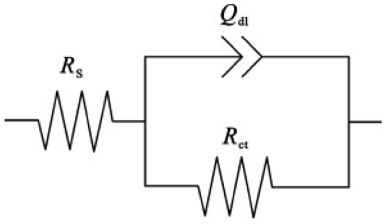

Fig. 3. Equivalent circuits compatible with the experimental impedance data in Fig. 2 for corrosion of steel electrode at different inhibitor concentrations.

Table 1. Impedance data for steel in 1 M HCl solution without and with different concentration of DHBP at 20 °C

Concentration / M	R_s / cm^2	R_{ct} / cm^2	Q_{dl} / F cm^{-2}	C_{dl} / F cm^{-2}	n	θ
Blank	1.9	77	0.0019	0.0013	0.85	-
1×10^{-4}	1.8	202	0.0016	0.0013	0.87	0.61
3×10^{-4}	1.9	285	0.0014	0.0012	0.87	0.72
5×10^{-4}	1.9	342	0.0013	0.0011	0.89	0.77
1×10^{-3}	2.1	517	0.0011	0.0010	0.91	0.85
2×10^{-3}	2.1	781	0.0010	0.0009	0.91	0.90

ments are obtained. Table 1 illustrates the equivalent circuit parameters for the impedance spectra of corrosion of steel in 1 M HCl Solution. The degree of surface coverage and the inhibition efficiency ($IE\% = \theta \times 100$) for different concentrations of inhibitor is calculated using the following equation [25]:

$$IE\% = \frac{R_{ct}^{-1} - R_{ct(inh)}^{-1}}{R_{ct}^{-1}} \times 100 \quad (2)$$

The charge transfer resistance increases with increasing inhibitor concentrations due to the higher inhibition efficiencies. The data indicate that increasing charge transfer resistance associates with a decrease in the double layer capacitance. The decrease in Q_{dl} values cause by adsorption of inhibitor indicates that the exposed surface area decreases. On the other hand, a decrease in Q_{dl}, which can result from a decrease in local dielectric constant and/or an increase in the thickness of the electrical double layer, suggests that the inhibitor acts by adsorption at the metal-solution interface and the formation of a protective layer on the electrode surface [18]. The thickness of this protective layer increases with the increase in inhibitor concentration, since more inhibitor will electrostatically adsorb on the electrode surface. This trend is in accordance with Helmholtz model, given by the following equation [10,18]:

$$C_{dl} = \frac{\varepsilon_0 \varepsilon S}{e} \quad (3)$$

where e is the thickness of the protective layer, ε is the dielectric constant of the medium, ε_0 is the vacuum permittivity and S is the effective surface area of the electrode.

As the Q_{dl} exponent (n) is a measure of the surface heterogeneity, values of n indicates that the steel surface becomes more and more homogeneous as the concentration of inhibitor increases as a result of its adsorption on the steel surface and corrosion inhibition. The increase in values of R_{ct} and the decrease in values of Q_{dl} with increasing the concentration also indicate that inhibitor acts as primary interface inhibitor and the charge transfer controls the corrosion of steel under the open circuit conditions.

3.2. Potential of zero charge

The adsorption of organic compounds on the metal surface generally depends on the surface charge of the metal and the charge or dipole moment of the inhibitor molecule and other ions that are specifically adsorbed on to the metal surface [26]. The surface charge of the metal is determined from the open circuit potential with respect to the PZC [27]. The dependency of the double layer capacitance on the applied dc potential is shown in the Fig. 4. The values of E_{ocp} and PZC for steel in the inhibited and uninhibited solutions are given in the Table 2. The surface charge of steel is found at the open circuit potential using the equation $E_r = E_{ocp} - E_{pzc}$, where E_r is antropov's rational corrosion potential [28]. The surface charge of steel at the OCP is found to be positive in the inhibited and uninhibited HCl solutions.

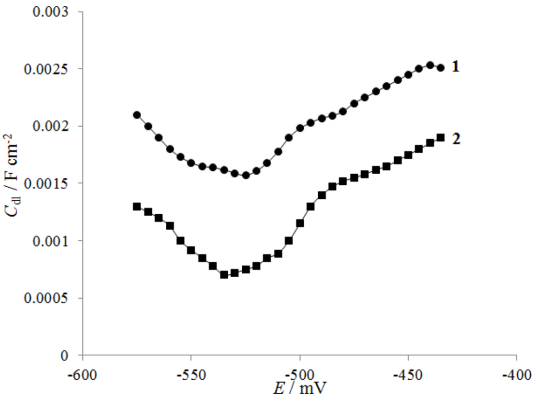

Fig. 4. The plot of differential capacitance vs. applied electrode potential in 1 M HCl solution (1) and 1 M HCl solution containing 1×10^{-3} M of the inhibitor (2).

Table 2. Excess charge on steel electrode in 1 M HCl solutions in the presence and absence of inhibitor.

Concentration /M	E_{ocp} / mV	E_{pzc} / mV	E_r / mV	Excess Charge
Blank	-501	-525	24	+
1×10^{-3}	-507	-535	28	+

In the presence of the inhibitor, the metal surface is positively charged with respect to PZC [27-29], hence chloride ions will first get adsorbed in the metal surface after that the protonated inhibitor molecules will be adsorbed and the metal ion dissolution will be effectively protected [30]. In the uninhibited HCl solution, the mechanism of anodic dissolution involves the reversible adsorption of the anion Cl^- on steel surface, release of electrons from the anions adsorbed onto the metal surface and desorption of adsorbed species with Fe^{+2} ions after picking up elec-

trons from the steel surface [27,29]. The inhibitor molecules existing in the protonated form through the heteroatoms N or O in HCl solution are in equilibrium with the corresponding molecular (unprotonated) form. Thus, it is very difficult for the positively charged inhibitor to approach the positively charged metal surface because of electrostatic repulsion. The protonated molecules can get adsorbed on the steel surface via Cl^- ions that form interconnecting bridges between the positively charged metal surface and the protonated organic inhibitors [31,32].

$$Fe + Cl^- \leftrightarrow (FeCl^-)_{ads} + Inh(FeCl^-Inh^+)_{ads}$$

In addition to this type of physical adsorption, the adsorption of inhibitor molecules may also take place through donor acceptor interactions between π electrons of $N = C$, benzene ring and the lone pair of electrons on *N*, *O* and *S* atoms present in the unprotonated form of inhibitor molecules and the vacant 'd' orbitals of surface iron atoms [23].

3.3. Adsorption isotherm

Adsorption isotherms provide information about the interaction of the adsorbed molecules with the metal surface [16]. The efficiency of schiff base molecules as a successful corrosion inhibitor mainly depends on their adsorption ability on the metal surface. The adsorption process consists of the replacement of water molecules at a corroding interface according to following process [33]:

$$Org_{(sol)} + nH_2O_{(ads)} \rightarrow Org_{(ads)} + nH_2O_{(sol)} \quad (4)$$

where $Org_{(sol)}$ and $Org_{(ads)}$ are the organic molecules in the solution and adsorbed on the metal surface, respectively, and n is the number of water molecules replaced by the organic molecules. It is essential to know the mode of adsorption and the adsorption isotherm. Different adsorption isotherms (Langmuir, Temkin, Freundlich, Frumkin, Modified Langmuir, Henry, Viral, Damaskin, Volmer and Flory-Huggins) [34,35] were tested for their fit to the experimental data. The linear regression coefficient values (R^2) determine from the plotted curves. According to these results, it can be concluded that the best description of the adsorption behavior of DHBP can be explained by Langmuir adsorption isotherm which is given by:

$$\frac{C}{\theta} = \frac{1}{K_{ads}} + C \quad (5)$$

where θ is the surface coverage degree, C is the concentration of inhibitor and K_{ads} is the adsorptive equilibrium constant. The linear relationships of $C\ \theta^{-1}$ versus C, depicted in Fig. 5 suggest that the adsorption of DHBP on the steel surface obey the Langmuir adsorption isotherm. Langmuir's isotherm assumes that the adsorption of organic molecule on the adsorbent is monolayer and the adsorbed molecules occupy only one site and there are no interactions with other adsorbed species. The standard free energy of adsorption of inhibitor (ΔG_{ads}) on steel surface can be evaluated with the following equation:

$$\Delta G_{ads} = -RT\ln(55.5K_{ads}) \quad (6)$$

The value 55.5 in the above equation is the concentration of water in solution in mol.l^{-1} [10]. The negative values of ΔG_{ads} suggest that the adsorption of DHBP on the steel surface is spontaneous. Generally, the values of ΔG_{ads} around or less than -30 kJ mol^{-1} are associated with the electrostatic interaction between charged molecules and the charged metal surface (physisorption); while those around or higher than -40 kJ mol^{-1} mean charge sharing or transfer from the inhibitor molecules to the metal surface to form a coordinate type of metal bond (chemisorption). The values of K_{ads} and ΔG_{ads} are 1.1×10^{-4} l mol^{-1} and -33.03 kJ mol^{-1}, respectively. The ΔG_{ads} values are around -30 kJ mol^{-1}, which means that

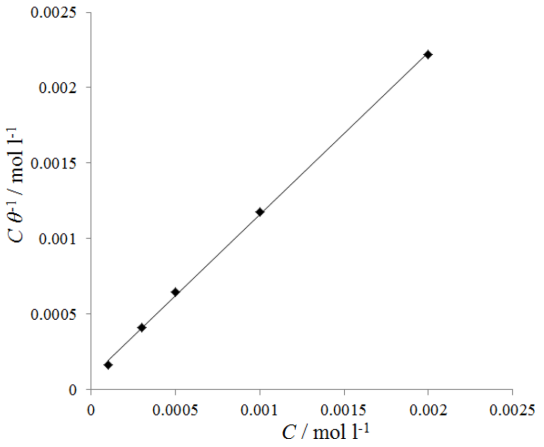

Fig. 5. Langmuir adsorption plot for steel electrode in 1 M HCl.

the absorption of DHBP on the steel surface belongs to the physisorption and the adsorptive film has an electrostatic character [11,16].

3.4. Potentiodynamic polarization

Potentiodynamic polarization was obtained for steel electrode in 1 M HCl solution with and without inhibitor. Polarization curves in various concentrations of DHBP in 1 M HCl solutions are presented in Fig. 6, at 20 °C. The polarization exhibits Tafel behavior. The corresponding electrochemical parameters, i.e., corrosion potential (E_{corr} versus SCE), corrosion current density (I_{corr}), cathodic and anodic Tafel slopes (β_a,β_c), polarization resistance (R_p) and the inhibition efficiency were obtained by extrapolation of the Tafel lines and are shown in Table 3. The addition of DHBP shifts both anodic and cathodic branches to the lower values of corrosion current densities and thus causes a remarkable decrease in the corrosion rate. It can be clearly seen from Fig. 6 that, both anodic metal dissolution of iron and cathodic hydrogen ions reduction reactions are inhibited after the addition of schiff base to the aggressive solution. These results are indicative of the adsorption of inhibitor molecules on steel surface. The inhibition of both anodic and cathodic reactions increases with the increasing inhibitor concentrations. The cathodic current-potential curves give rise to parallel lines indicates that the addition of DHBP to the 1 M HCl solution does not modify the reduction mechanism. The corrosion potential shows a small change in the range of -495 to -505 mV vs. SCE. These results indicated that the presence of DHBP compound inhibits iron oxidation and the hydrogen evolution reaction. Consequently these compounds can be classified as the mixed corrosion inhibitors, as electrode potential displacement is lower than 85 mV in any direction [36]. The polarization resistance (R_p) from Tafel extrapolation method is calculated using the Stern-Geary equation [37]:

$$R_p = \frac{\beta_a \cdot \beta_c}{2.303(\beta a + \beta c)} \frac{1}{I_{corr}} \quad (7)$$

By increasing the inhibitor concentration, the polarization resistance increases in the presence of compound, indicating adsorption of the inhibitor on the metal surface to block the active sites efficiently and inhibit corrosion which is in agreement with impedance spectroscopy results.

3.4. Surface studies

In order to evaluate the conditions of the steel sur-

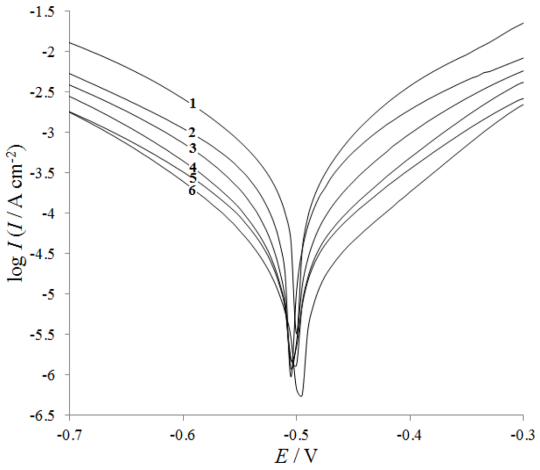

Fig. 6. Anodic and cathodic polarization curves of steel in 1 M HCl without and with various concentration of DHBP at 20 °C: (1) 0, (2) 1×10^{-4}, (3) 3×10^{-4}, (4) 5×10^{-4}, (5) 1×10^{-3}, (6) 2×10^{-3} M.

Table 3. Potentiodynamic polarization parameters for the corrosion of steel in 1 M HCl solution in absence and presence of different concentrations of DHBP at 20 °C.

Concentration / M	I_{corr} / μA cm^{-2}	$-E_{corr}$ / V	β_a / V dec^{-1}	$-\beta_c$ / V dec^{-1}	R_p / Ω cm^{-2}	*IE* %
Blank	323	-0.501	0.105	-0.102	69.42	-
1×10^{-4}	177.8279	-0.505	0.117	-0.086	121.03	45
3×10^{-4}	93.32543	-0.504	0.115	-0.093	239.23	71
5×10^{-4}	52.48075	-0.502	0.108	-0.099	427.36	83
1×10^{-3}	30.90295	-0.505	0.139	-0.122	912.93	90
2×10^{-3}	17.78279	-0.495	0.145	-0.119	1595.94	94

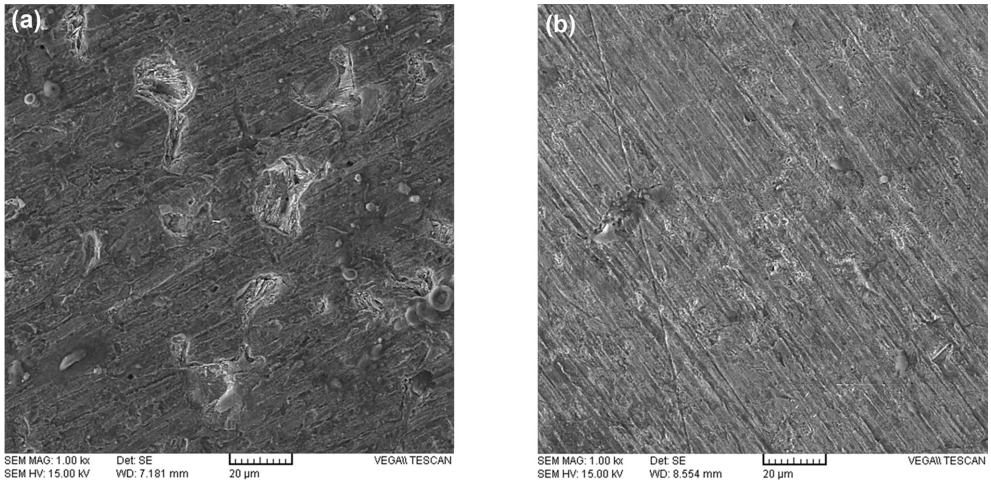

Fig. 7. Surface of steel electrode by SEM microscope at in 1 M HCl solution : (a) without and (b) with 1×10^{-3} M DHBP.

faces in contact with hydrochloric acid solution, surface analysis was carried out. Surface was observed after 6 h of immersion in 1 M HCl in the absence and presence of DHBP. Scanning electron microscopy (SEM) images of the surface in the absence and presence of inhibitor are presented in Fig. 7. The SEM images reveal the presence of corrosion attack and some pits on the surface in the absence of inhibitor while such damages diminish in the presence of inhibitor. As can be seen from these figures, it is obvious that the surface looks more uniform in the presence of inhibitor.

4. Conclusion

The Schiff base was synthesized and investigated as corrosion inhibitor for API-5L-X65 steel in 1 M HCl solution using electrochemical techniques. The following conclusions were drawn:

1. Schiff base had high inhibition effect for the corrosion of API-5L-X65 steel in 1 M HCl solution especially in high concentration. The high inhibition efficiency of Schiff base attributed to the formation of a film on the steel surface.

2. Impedance measurements indicated that with increasing inhibitor concentration, the charge transfer resistance increased, while the double-layer capacitance decreased.

3. The adsorption of Schiff base molecules on steel surface was described by Langmuir adsorption isotherm. The values of ΔG_{ads} and K_{ads} indicated the spontaneous interaction with surface and high adsorption ability of studied inhibitor.

4. Determination of PZC values indicated that the inhibitor molecules get adsorbed on the metal surface via chloride bridge.

5. The PZC values and the value of ΔG_{ads} calculated from adsorption isotherm showed that the adsorption mechanism is physisorption.

6. Polarization measurements demonstrate that Schiff base behaved as mixed type corrosion inhibitor by inhibiting both anodic metal dissolution and cathodic reaction.

7. The scanning electron microscopy micrographs showed that the steel surface was corroded in 1 M HCl solution and the addition of inhibitor to the aggressive solutions diminished the corrosion of steel.

Refrerences

[1] J. K. Odusote and O. M. Ajayi, *J. Electrochem. Sci. Technol.*, **2013**, *4*, 81-87.
[2] M. A. Hegazy, M. Abdallah, M. K. Awad and M. Rezkm, *Corros. Sci.,* **2014**, *81*, 54-64.
[3] M. A. Migahed, A. M. Al-Sabagh, E. A. Khamis and E. G. Zaki, *J. Mol. Liq.,* **2015**, *212*, 360-371.
[4] A. S. Fouda, M. T. Mohamed and M. R. Soltan, *J. Electrochem. Sci. Technol.*, **2013**, *4*, 61-70.
[5] Z. Moallem, I. Danaee and H. Eskandari, *Trans. Indian Inst. Met.,* **2014**, *67*, 817-825.
[6] A. Karimi, I. Danaee, H. Eskandari and M. RashvanAvei, *Prot. Met. Phys. Chem. Surf.,* **2015**, *51*, 899-907.
[7] A. S. Fouda, A. M. El-Defrawy and M. W. El-Sherbeni,

J. Electrochem. Sci. Technol., **2013**, *4*, 47-56.
[8] I. Danaee, O. Ghasemi, G. R. Rashed, M. RashvandAvei and M. H. Maddahy, *J. Mol. Struct.*, **2013**, *1035*, 247-259.
[9] A. A. Gürten, H. Keleº, E. Bayol and F. Kandemirli, *J. Ind. Eng. Chem.*, **2015**, *27*, 68-78.
[10] H. M. Abd El-Lateef, A. M. Abu-Dief, L. H. Abdel-Rahman, E. C. Sañudo and N. Aliaga-Alcalde, *J. Electroanal. Chem.,* **2015**, *743*, 120-133.
[11] T. K. Chaitra, K. N. S. Mohana and H. C. Tandon, *J. Mol. Liq.,* **2015**, *211*, 1026-1038.
[12] N. K. Gupta, C. Verma, M. A. Quraishi, A. K. Mukherjee, *J. Mol. Liq.,* **2016**, *215*, 47-57.
[13] S. A. Fairhurst, D. L. Hughes, U. Kleinkes, G. L. Leigh, J. R. Sanders and J. Weisner, *J. Chem. Soc. Dalton Trans.,* **1995**, *3*, 321-326.
[14] J. R. Macdonald, *Solid State Ion.,* **1984**, *13*, 147-149.
[15] I. Danaee, *J. Electroanal. Chem.,* **2011**, *662*, 415-420.
[16] H. Jafari, I. Danaee, H. Eskandari and M. RashvandAvei, *Ind. Eng. Chem. Res.*, **2013**, *52*, 6617-6632.
[17] L. Larabi, Y. Harek, M. Traianel and A. Mansri, *J. Appl. Electrochem.,* **2004**, *34*, 833-839.
[18] A. R. Hoseinzadeh, I. Danaee and M. H. Maddahy, *J. Mater. Sci. Technol.*, **2013**, *29*, 884-892.
[19] I. Danaee, M. Gholami, M. RashvandAvei and M. H. Maddahy, *J. Ind. Eng. Chem.,* **2015**, *26*, 81-94.
[20] S. Martinez and M. Metikoš-Hukovic´, *J. Appl. Electrochem.,* **2003**, *33*, 1137-1142.
[21] F. Bentiss, M. Lebrini, H. Vezin, F. Chai, M. Traisnel and M. Lagrené, *Corros. Sci.,* **2009**, *51*, 2165-2173.
[22] I. Danaee and S. Noori, *Int. J. Hydrogen Energy*, **2011**, *36*, 12102-12111.
[23] M. Gholami, I. Danaee, M. H. Maddahy and M. Rashvandavei, *Ind. Eng. Chem. Res.*, **2013**, *52*, 14875-14889.
[24] S. RameshKumar, I. Danaee, M. RashvandAvei and M. Vijayan, *J. Mol. Liq.,* **2015**, *212*, 168-186.
[25] A. Yurt, B. Duran and H. Dal, *Arab. J. Chem.*, **2014**, *7*, 732-740.
[26] H. Ma, S. Chen, B. Yin, S. Zhao and X. Liu, *Corros. Sci.,* **2003**, *45*, 867-882.
[27] R. Solmaz, M. E. Mert, G. Kardas, B. Yazici and M. Erbil, *Acta Physico -Chimica Sinica,* **2008**, *24*, 1185-1191.
[28] A. Popova, E. Sokolova, S. Raicheva and M. Christov, *Corros. Sci.,* **2003**, *45*, 33-58.
[29] R. Solmaz, G. Kardas, M. Culha, B. Yazici and M. Erbil, *Electrochim. Acta,* **2008**, *53*, 5941-5952.
[30] K. Mallaiya, R. Subramaniam, S. Sathyamangalam Srikandan, S. Gowri, N. Rajasekaran and A. Selvaraj, *Electrochim. Acta,* **2011**, *56*, 3857-3863.
[31] I. Tang, X. Li, G. Mu and G. Liu, *Surf. Coat. Technol.,* **2006**, *201*, 384-388.
[32] R. Solmaz, G. Kardas, B. Yazici and M. Erbil, *Colloids Surf. A Physicochem. Eng. Asp.,* **2008**, *312*, 7-17.
[33] E. E. Oguzie, C. Unaegbu, C. N. Ogukwe, B. N. Okolue and A. I. Onuchukwu, *Mater. Chem. Phys.,* **2004**, *84*, 363-368.
[34] A. R. Hoseinzadeh, I. Danaee, M. H. Maddahy and M. RashvandAvei, *Chem. Eng. Comm.,* **2014**, *201*, 380-402.
[35] G. Mu, X. Li, Q. Qu and J. Zhou, *Corros. Sci.,* **2006**, *48*, 445-459.
[36] M. M. Saleh and A. A. Atia, *J. Appl. Electrochem.,* **2006**, *36*, 899-905.
[37] H. Gerengi and H. I. Sahin, *Ind. Eng. Chem. Res.,* **2012**, *51*, 780-787.